ORIGINAL RESEARCH

Docetaxel-loaded multilayer nanoparticles with nanodroplets for cancer therapy

Keun Sang Oh[1],*
Kyungim Kim[1],*
Byeong Deok Yoon[1]
Hye Jin Lee[1]
Dal Yong Park[1]
Eun-yeong Kim[1]
Kiho Lee[1]
Jae Hong Seo[2]
Soon Hong Yuk[1,2]

[1]College of Pharmacy, Korea University, Sejong, [2]Biomedical Research Center, Korea University Guro Hospital, Guro-gu, Seoul, Republic of Korea

*These authors contributed equally to this work

Correspondence: Soon Hong Yuk
College of Pharmacy, Korea University, 2511 Sejongro, Sejong 339-700, Republic of Korea
Tel +82 44 860 1612
Fax +82 44 860 1606
Email shyuk@korea.ac.kr

Abstract: A mixture of docetaxel (DTX) and Solutol® HS 15 (Solutol) transiently formed nanodroplets when it was suspended in an aqueous medium. However, nanodroplets that comprised DTX and Solutol showed a rapid precipitation of DTX because of their unstable characteristics in the aqueous medium. The incorporation of nanodroplets that comprised DTX and Solutol through vesicle fusion and subsequent stabilization was designed to prepare multilayer nanoparticles (NPs) with a DTX-loaded Solutol nanodroplet (as template NPs) core for an efficient delivery of DTX as a chemotherapeutic drug. As a result, the DTX-loaded Solutol nanodroplets (~11.7 nm) were observed to have an increased average diameter (from 11.7 nm to 156.1 nm) and a good stability of the hydrated NPs without precipitation of DTX by vesicle fusion and multilayered structure, respectively. Also, a long circulation of the multilayer NPs was observed, and this was due to the presence of Pluronic F-68 on the surface of the multi-layer NPs. This led to an improved antitumor efficacy based on the enhanced permeation and retention effect. Therefore, this study indicated that the multilayer NPs have a considerable potential as a drug delivery system with an enhanced therapeutic efficacy by blood circulation and with low side effects.

Keywords: multilayer nanoparticles, Solutol, Pluronic F-68, docetaxel, cancer therapy

Introduction

The assembly of nanoparticles (NPs) into multilayer films has been studied to overcome intrinsic drawbacks in the release kinetics and the stability of NPs in an aqueous medium. This has been demonstrated with the incorporation of NPs into the vesicles (liposomes) to form lipid bilayer-supported NPs.[1–3] If lipid vesicles (liposomes) coexist with one another under similar circumstances, they can form a new, larger one. Because vesicles open adjacent and contacted on lipid bilayers through the fusion process, the leak of captured cargos was typically observed.[4,5] On the other hand, vesicles may capture foreign substances when there is an attractive interaction between the vesicles and the foreign substances, such as NPs.[6] Another strategy has been designed and characterized based on a layer-by-layer approach through various interactions, such as hydrogen bonding, electrostatic interaction, and chemical bonding.[7,8] These have led to the formation of various types of multilayer NPs with significant progress in drug delivery applications.[9–14]

Solutol® HS 15 (Solutol) consists of polyglycol mono- and diester of 12-hydroxy-stearic acid with polyethylene glycol and free polyethylene glycol. Due to the presence of lipophilic ester, Solutol has been used in the aqueous parenteral preparation for lipophilic pharmaceutical active agents.[15,16]

In this study, docetaxel (DTX), a member of the taxane drug class, has been used as a hydrophobic model drug and has become an anticancer drug with an approved
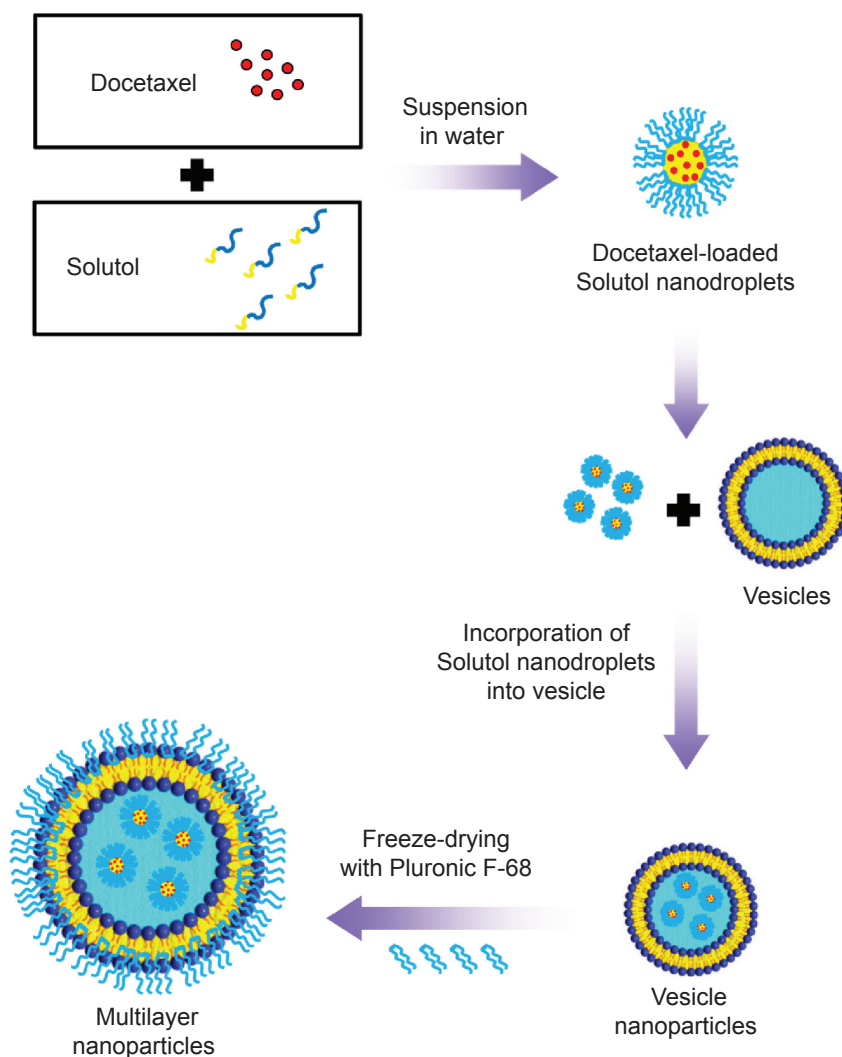
Figure 1 Schematic description of the formation of multilayer NPs.
Abbreviation: NPs, nanoparticles.

clinical efficacy against various solid tumors (breast, non-small-cell lung, and prostate cancers).[17,18] Recently, DTX was prepared as Tween 80-based parenteral dosage (as the generic name Taxotere®) with more enhanced solubility than free DTX in an aqueous condition. However, the administration of DTX in that formulation led to adverse side effects, including neutropenia, hair loss, allergic reactions, fatigue, and muscle discomfort, because of either the active agents or the excipients (Tween 80 and residual ethanol).[18–20]

Because of the lipophilic characteristics of DTX and Solutol, they mix to form a homogeneous phase. When the DTX dissolved in Solutol (transparent mixture) was suspended in an aqueous medium, it formed DTX-loaded Solutol nanodroplets, which maintained their nanostructure for a short period of time. In this study, an improvement in the stability of DTX-loaded Solutol nanodroplets in an aqueous medium was made through

vesicle fusion. Further stabilization was carried out using the interaction between Pluronic F-68 and lipid bilayer, and a new delivery system for DTX was prepared in a powdery form. Figure 1 describes the fusion process of DTX-loaded Solutol nanodroplets into the vesicles and subsequent stabilization of the vesicles with Pluronic F-68 to form multilayer structured NPs (multilayer NPs) in a solid form. We then measured drug release behavior and cytotoxicity of the NPs. Finally, the therapeutic efficacy of the multilayer NPs was observed by evaluating tumor growth inhibition in tumor xenograft mice models after intravenous injections.

Materials and methods
Materials
Pluronic F-68, $(PEO)_{79}(PPO)_{28}(PEO)_{79}$ amphiphilic triblock copolymer (average molecular weight =8,350 g/mol), and

Solutol (polyoxyl 15 hydroxy stearate) were obtained from BASF Corporation, Republic of Korea, and were used as received. DTX (in anhydrous form) was purchased from Parling Pharma Tech Co., Ltd. (Shanghai, People's Republic of China). L-Phosphatidylcholine from soybean, Nile red, and Rhodamine B were purchased from Sigma-Aldrich Co. (St Louis, MO, USA). C3H/HeN mice (male 5.5 weeks old, 20–25 g) were purchased from Nara Biotech (Pyeongtaek, Republic of Korea).

Methods

Preparation of the multilayer NPs

For the preparation of DTX-loaded Solutol nanodroplets, weighed amounts of DTX and Solutol were prepared and mixed to form a homogeneous phase. Solutol containing DTX was suspended in distilled–deionized water (DI water) to obtain the suspension of DTX-loaded Solutol nanodroplet NPs (10 wt% of DTX-loaded Solutol nanodroplets in an aqueous solution). For the preparation of vesicle type, an aqueous condition (20 wt%) of L-α-phosphatidylcholine was prepared by a probe-type ultrasonic processor (VCX-750; Sonics & Materials, Newtown, CT, USA).

To prepare the vesicle NPs, equal amounts of the suspensions of DTX-loaded Solutol nanodroplets were mixed with the lipid vesicle suspension, and 10 wt% of the Pluronic F-68 in DI water was mixed with the prepared vesicle NPs at a weight ratio of 60/40 (w/w). Finally, the solution mixture was lyophilized to form a polymeric shell on the surfaces of the vesicle NPs. Trehalose as a cryo-protectant (5 wt% of total of the lipid vesicles) was used with Pluronic F-68 solution to maintain morphology and particle size of the NPs during lyophilization.[21,22]

To observe the cellular uptake behavior of the multilayer NPs, Nile red and Rhodamine B were loaded during the formation of multilayer NPs, as described in Figure 2. Because of the hydrophobic nature of Nile red, it was loaded with DTX in the Solutol phase. Positively charged hydrophilic Rhodamine B was mixed with lecithin aqueous solution and embedded outside the Solutol phase after freeze-drying.

Physicochemical characteristics of NPs

The average diameter and size distribution of the NPs (1 mg/mL of NPs dispersed in phosphate-buffered saline [PBS, pH 7.4]) were measured with a particle size analyzer (Zeta Sizer Nano Series; Malvern Instruments, Malvern, UK). The particle morphology was observed with transmission electron microscopy (TEM) (FEI Tecnai G^2; FEI Company, Hillsboro, OR, USA). To prepare the samples, 10 μL of the dispersed NPs in distilled–DI water was poured on a carbon-coated TEM grid

with 300 mesh and then stained with 2 wt% uranyl acetate for negative staining at room temperature for ~12 hours.

Also, the hydrated vesicle NPs were observed in the vesicular morphologies using cryogenic TEM (Cryo Tecnai F20 G^2; FEI Co.). For the cryogenic TEM measurement, ~7 mL of the dispersed NPs in DI water was prepared as a thin aqueous film supported on a cryo-grid, and the excess hydrated NPs were removed by blotting onto a filter paper. The images were performed at −170°C using a Multiscan 600 W CCD camera (Gatan, Inc., Warrendale, PA, USA).

In vitro drug release characteristics of NPs

To observe the release behavior of DTX from NPs, 10 mg of the DTX-loaded multilayer NPs (DTX multilayer NPs) were dispersed in 4 mL of PBS (pH 7.4) containing 0.1% (w/v) Tween 80 to maintain the sink conditions. This was then put into a dialysis membrane bag of MWCO of 12–14 kDa (Spectrum® Laboratory, Rancho Dominguez, CA, USA), which was immersed in a conical centrifuge tube with 15 mL of PBS. The dialysis membrane with multilayer NPs was placed in a water bath maintained at 37°C and shaken horizontally at 150 rpm. Subsequently, 1.5 mL of the released buffer was withdrawn at predetermined time intervals, and the total released buffer was replaced with the equal volume of fresh PBS to maintain the sink conditions. Released DTX concentration in the buffer was determined from the standard curve constructed from serial dilutions of DTX by HPLC (Agilent 1100 Series; Agilent Technologies, Santa Clara, CA, USA) using an Agilent ZORBAX Eclipse XDB C18 column (250 mm ×4.6 mm, 5 μm) and an acetonitrile/water (60/40, v/v) mobile phase over 10 minutes at a flow rate of 0.8 mL/min. The eluent was monitored by UV detector at 220 nm.

In vitro cytotoxicity and cellular uptake behavior of the NPs

SCC-7 (murine squamous cell carcinoma) cells were cultured in RPMI-1640 media supplemented with 10% FBS, 100 U/mL penicillin, and 100 μg/mL streptomycin at 37°C in the CO$_2$ incubator.

The cytotoxicity of the commercial DTX formulation with Tween 80 and ethanol (Taxotere®), bare NPs, DTX-loaded vesicle NPs (DTX vesicle NPs), and DTX multilayer NPs was evaluated by cell proliferation assay using a cellular metabolic activity of 3-(4,5-dimethylthiazol-2-yl)-2,5-diphenyltetrazolium bromide. The cells were seeded at a density of 5×10^3 cells to each well in 96-well plates and further incubated to adhere for ~24 hours. The cells were washed with fresh PBS twice and incubated for 24 hours or
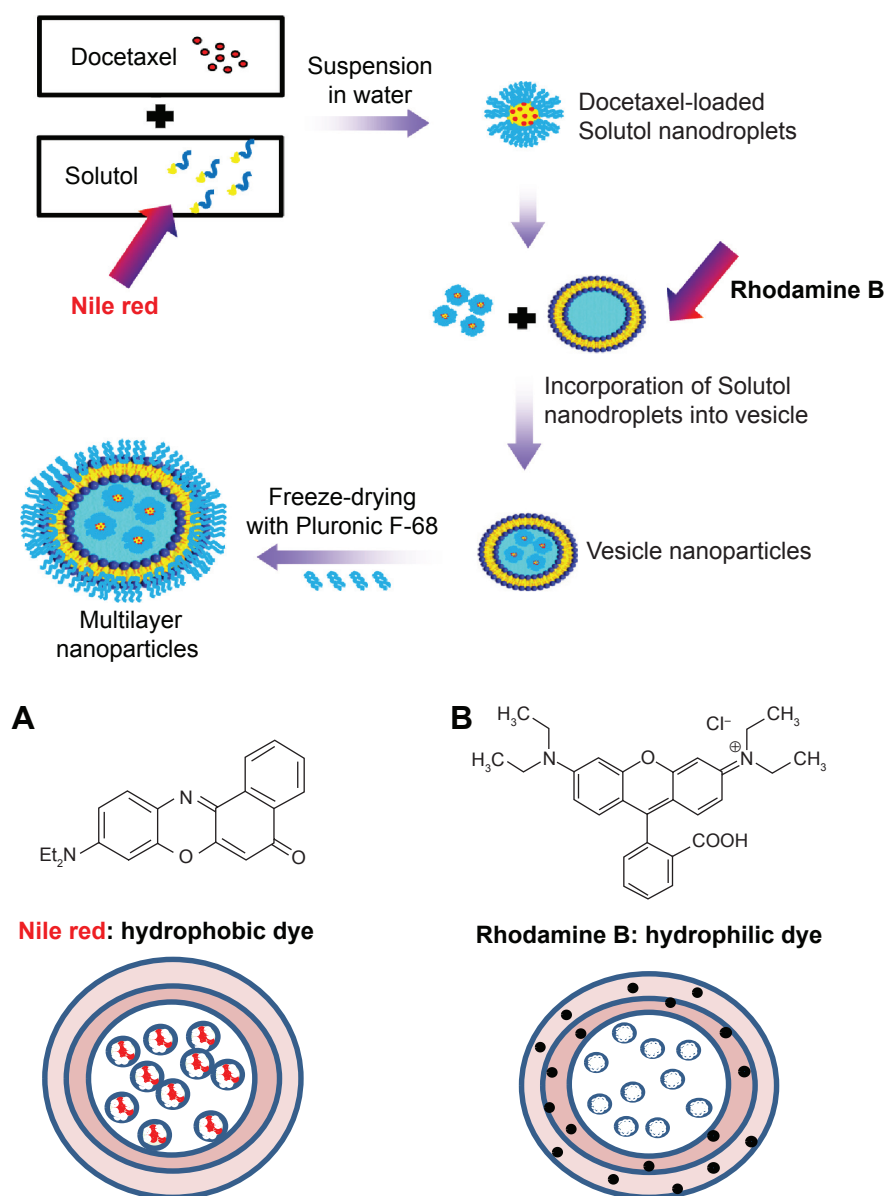
Figure 2 Schematic description of the multilayer NPs.
Notes: (**A**) DTX and Nile red (hydrophobic dye) and (**B**) DTX and Rhodamine B (hydrophilic dye).
Abbreviations: DTX, docetaxel; NPs, nanoparticles.

48 hours with serial dilutions of various drug formulations (commercial DTX formulation, bare NPs, DTX vesicle NPs, and DTX multilayer NPs). The cells were then washed with fresh PBS twice to remove the excess samples. Twenty-five microliters of 3-(4,5-dimethylthiazol-2-yl)-2,5-diphenyltetrazolium bromide solution (1 mg/mL in PBS) was added to each well, and the cells were incubated for 2 hours in the CO_2 incubator. Two hundred microliters of dimethyl sulfoxide was then added to the cells to solubilize the precipitated formazan crystals with purple color for ~30 minutes on a horizontal shaker. Absorbance was measured using a UV–Vis microplate reader (VERSAmax™; Molecular Devices LLC, Sunnyvale, CA, USA) at 570 nm.

For observing cellular internalization of DTX multilayer NPs, the cells were seeded at a density of 5×10^3 cells in 35 Ø flat-bottomed dishes with coverslip, allowed to adhere for 24 hours, and then treated with the multilayer NPs containing Nile red or Rhodamine B to a final concentration of 100 µM. The cells were incubated for four additional times (0.5 hour, 1 hour, 2 hours, and 4 hours) with the multilayer NPs and washed with fresh PBS twice to remove the excess NPs. The cells were then fixed at room temperature in 4% (v/v) paraformaldehyde solution for 30 minutes. After washing with PBS twice, the cells were treated with 4′,6-diamidino-2-phenylindole to stain the nuclei. Finally, the cellular uptake was observed using a fluorescent microscope (Axio Observer;

Carl Zeiss Meditec AG, Jena, Germany) to visualize 4′,6-diamidino-2-phenylindole (345/661 nm), the multilayer NPs containing Nile red (510/595 nm), and the multilayer NPs containing Rhodamine B (557/571 nm).

Pharmacokinetic (PK) studies of NPs

ICR mice (male, 8 weeks old, 30–35 g; ORIENT BIO Inc., Seongnam-si, Republic of Korea) were adapted to the testing facility for approximately a week prior to the study. DTX dissolved in dimethylacetamide/Tween 80/saline (10/5/85, v/v%) at 1 mg/mL was intravenously injected through the tail vein at a dose of 5 mg/kg. DTX formulations dissolved in normal saline at 1 mg DTX/mL were injected in the same manner at a dose of 5 mg/kg. Approximately 100 μL of blood samples were collected into BD Microtainer® plasma separator tubes at predetermined times through the saphenous vein over 24 hours postdosing. Blood samples were centrifuged at $6,000 \times g$ for 5 minutes to separate plasma. Plasma protein precipitation was conducted on 15 μL aliquots of plasma samples with three volumes of acetonitrile containing paclitaxel as internal standard. After centrifugation, the supernatant was analyzed by LC–MS/MS system (Agilent 6460 LC-QQQ; Agilent Technologies).

PK study was performed by using Phoenix WinNonlin (Version 3.1; Pharsight Corporation, St Louis, MO, USA). The elimination half-life ($t_{1/2}$) and the area under the curve (AUC) after administration by infusion were observed values from the experimental data and were plotted to the noncompartment modeling.

In vivo antitumor efficacy studies of the DTX NPs

The tumor xenograft mice model was performed as follows. Freshly harvested SCC-7 cells (1.0×10^6 cells/mouse) (n=4) were subcutaneously injected into the right flank of C3H/HeN athymic mice (male, 5.5 weeks old). When the tumor volume reached ~50–80 mm³, mice were administered an intravenous injection through the tail vein. The mice were randomly divided into one negative control group and four groups (n=4, 10 mg DTX/kg) as follows: 1) PBS (the control group), 2) commercial DTX formulation (Taxotere®), 3) bare multilayer NPs (with equivalent dosage as DTX multilayer NPs), 4) DTX vesicle NPs, and 5) DTX multilayer NPs. Each sample was intravenously injected through the tail vein once every 3 days for 12 days. Tumor volumes were measured using a digital vernier caliper and calculated using the following formula: tumor volumes = (length × width²/2). Also, the toxicity of each administered sample was evaluated by monitoring body weight changes. The mice were cared for according to the guidelines issued by the National Institute

of Health for the care and use of laboratory animals (NIH publication 80–23, revised in 1996). Animals were housed in groups of four or five under an alternating 12 hours light/dark cycle (lights on at 6 am), allowed food and water ad libitum, and were acclimatized for 7 days. This study was approved by the Ethical Committee on Animal Experimentation at Korea University, Republic of Korea.

Statistical analysis

The data are expressed as the mean ± SD of at least three experiments. Statistical differences were determined using the ORIGIN® 8.0 software program (OriginLab Corporation, Northampton, MA, USA). Statistical analysis was carried out using one-way analysis of variance (ANOVA), and in all cases, a P-value <0.05 was considered to be statistically significant, as noted in figures with asterisks.

Results and discussion
Preparation and characterization of the multilayer NPs

DTX-loaded Solutol nanodroplets, which are used as template NPs, were prepared by mixing Solutol and DTX to form a homogeneous mixture with subsequent addition of water. Because of a lipophilic nature, the Solutol formed a homogeneous mixture with DTX, and the mixture was suspended as nanodroplets for a certain period of time (Figure 3).

Figure 3C shows the size change of DTX Solutol nanodroplets as a function of time. When the mixture of Solutol and DTX was suspended in water, it formed the nanodroplets with an average diameter of ~11.7 nm (Figure 3A and B). However, a significant increase in diameter was observed after 3 hours with the precipitation of DTX (Figure 3C). With the penetration of water into the nanodroplets, the solubility of DTX in Solutol decreased, and the aggregation of DTX in the Solutol resulted in the increase in size of the nanodroplets for the first 5 hours. After that, precipitation of aggregated DTX from the nanodroplets was observed with a decrease in size of the nanodroplets.

To control the precipitation of DTX from the DTX Solutol nanodroplets, the template NPs were incorporated into the lipid vesicles to form the vesicle NPs. Subsequent stabilization was performed by lyophilization of the vesicle NPs in the presence of Pluronic F-68 to form the multilayer NPs (loading amount of DTX: 2.89±0.23 wt% and loading efficiency: 85.43±3.12 wt%). The formation of vesicle NPs was already reported previously.[3] As mentioned earlier, when lipid vesicles (liposomes) coexist with one another under similar circumstances, they can form a new, larger vesicle. Because vesicles open adjacent and contacted on lipid bilayers during the fusion process, Solutol nanodroplets
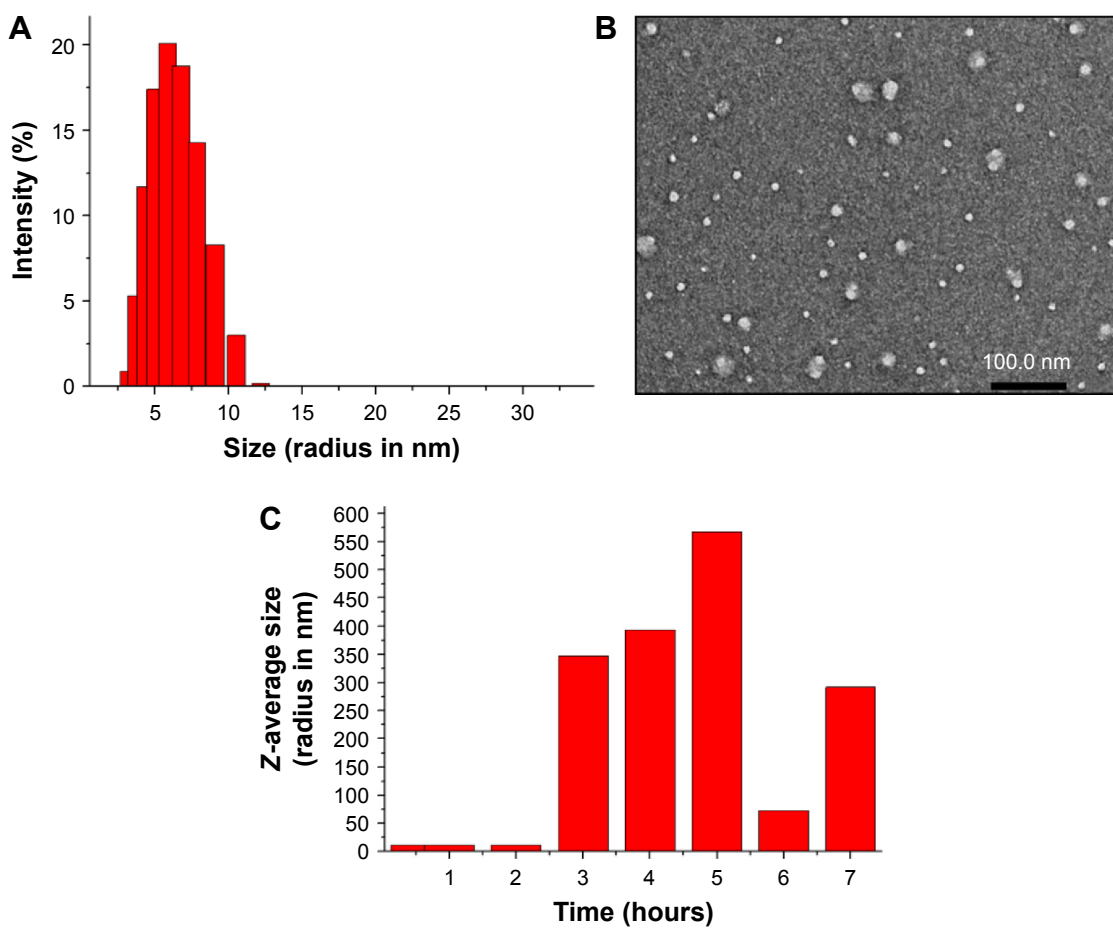
Figure 3 Physicochemical characteristics of the multilayer NPs.
Notes: (**A**) Size distribution of DTX-loaded Solutol nanodroplets (template NPs), (**B**) TEM image of template NPs, and (**C**) the change of NPs' size as a function of time.
Abbreviations: DTX, docetaxel; NPs, nanoparticles; TEM, transmission electron microscopy.

with DTX were incorporated into lipid vesicles to form the vesicle NPs (Figure 4C).

It has been reported that the hydrophobic chains (ie, polypropylene oxide portions) enabled Pluronics to physically anchor to the surface of the lipid bilayer membrane during lyophilization.[21–24] This interaction allowed the multilayered structure of the NPs as shown in Figure 4D. With the serial addition of lipid bilayer and Pluronic layer, the diameter of the NPs increased from 11.7 nm to 156.1 nm. The multilayer NPs did not show a change in their diameter during the 7 days in the aqueous medium.

In vitro release characteristic of DTX from the NPs

The in vitro release behavior of DTX from the NPs was observed using a dialysis system (Figure 5). Although template NPs maintained their nanostructure for 3 hours, much (45%) of the loaded DTX in the template NPs was released within 3 hours, with the precipitation of DTX in the release media. This was because of instability of the Solutol

nanodroplets, which are the main component of the template NPs. The sustainability of the release pattern became apparent with the addition of layers. Adding layers to template NPs to form the multilayer NPs, such as alternately adding lipid bilayer or Pluronic F-68, meant that these layers controlled the release rate of DTX.

In vitro cytotoxicity and cellular uptake of NPs

The cytotoxicity (cell death) of the free DTX (commercial DTX formulation [Taxotere®]), bare multilayer NPs, DTX vesicle NPs, and DTX multilayer NPs in cell culture media was assessed by determining the drug-loading effects on the viability of SCC-7 cells (n=6) (Figure 6). As expected, the bare NPs (multilayer NPs without DTX) showed a cell viability of almost 100% at 250 μg/mL, indicating a good cytocompatibility (low toxicity) in the cell culture system. In addition, the cytotoxicity of the free DTX, the vesicle NPs, and the multilayer NPs showed a significant dose-dependent cytotoxicity against SCC-7 cells. The DTX concentration
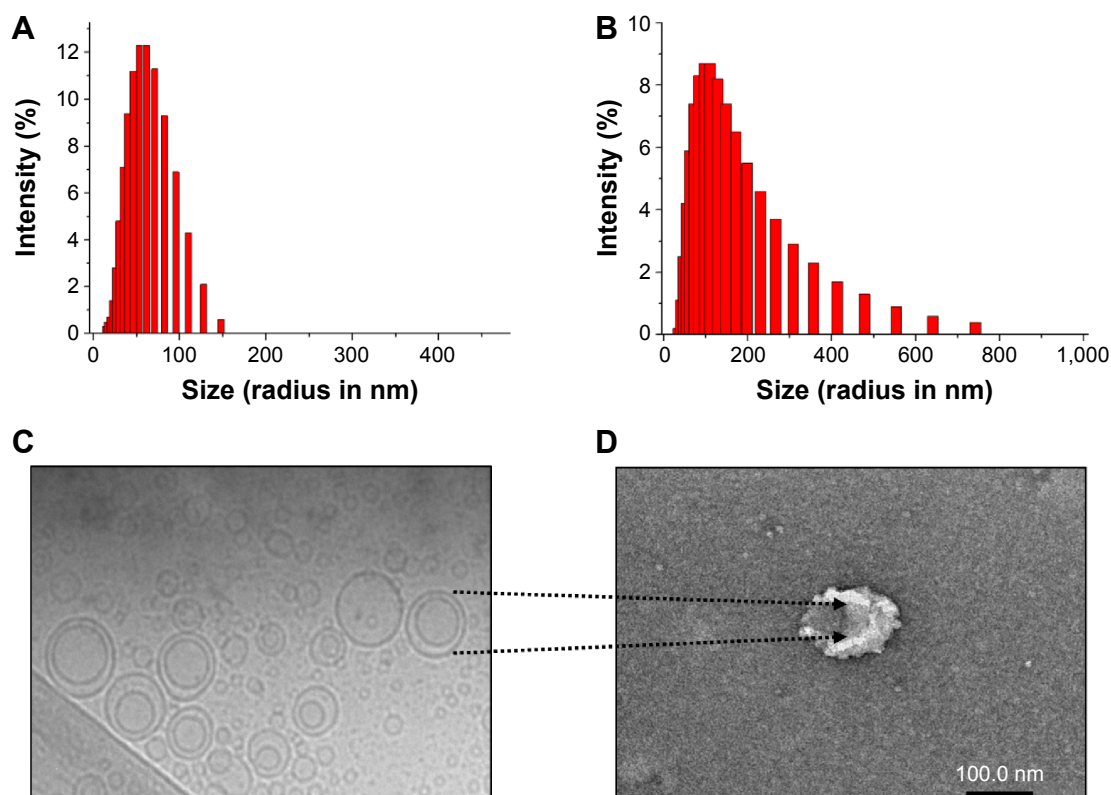
Figure 4 Particle size distribution and morphology of the NPs.
Notes: Size distribution of (**A**) DTX vesicle NPs, (**B**) DTX multilayer NPs, (**C**) cryo-TEM image of DTX vesicle NPs, and (**D**) TEM image of DTX multilayer NPs.
Abbreviations: cryo-TEM, cryogenic transmission electron microscopy; DTX, docetaxel; NPs, nanoparticles; TEM, transmission electron microscopy.

in NPs was gradually increased, and the cytotoxicity of the vesicle NPs and the multilayer NPs was significantly lower than that of the free DTX at most concentrations (Figure 6A). Because of the higher release rate of DTX from the vesicle NPs during a 1-day period, the cell viability of the vesicle NPs was lower when compared to that of the multilayer NPs. The lowest cell viability was observed

at the highest concentration of DTX after treatment for 2 days, which verified the sustained release of DTX from the multilayer NPs (Figure 6B).

To understand the mechanism of action by disrupting the microtubular network of DTX in cancer cells, the cellular uptake was observed using a fluorescence microscope. For this purpose, DTX multilayer NPs containing Nile red or Rhodamine B were prepared as described in Figure 2. Nile red is hydrophobic and compatible with Solutol.[25] Therefore, Nile red is expected to be localized in the Solutol core of multilayer NPs. Rhodamine B is hydrophilic and has strong interaction with the lipid bilayer.[26] Therefore, Rhodamine B is expected to be localized in the lipid bilayer and Pluronic shell of multilayer NPs. As shown in Figure 7A and B, rapid cellular uptake of multilayer NPs was observed irrespective of dyes, and the similar pattern of cellular uptake indicated that most of the DTX moved to the cytosol during the cellular uptake of multilayer NPs.

These DTX multilayer NPs may minimize the adverse effects of the current free DTX formulation containing Tween 80 and residual ethanol, such as anaphylaxis and severe hypersensitivity.[19,20] Furthermore, systemically prolonged
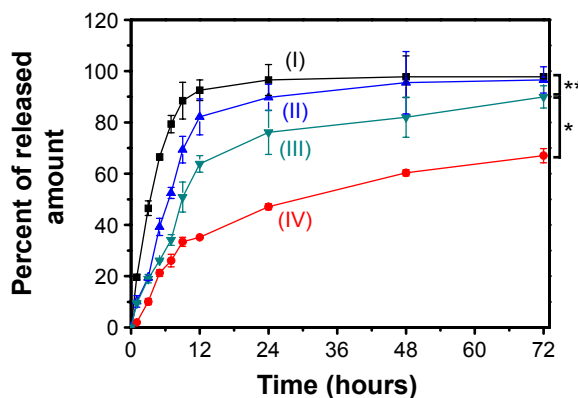

Figure 5 In vitro drug release characteristics.
Notes: (I) Template NPs, (II) free DTX, (III) the vesicle NPs, and (IV) the multilayer NPs. Data are presented as the mean ± SD (n=4). *$P>0.05$; **$P<0.05$.
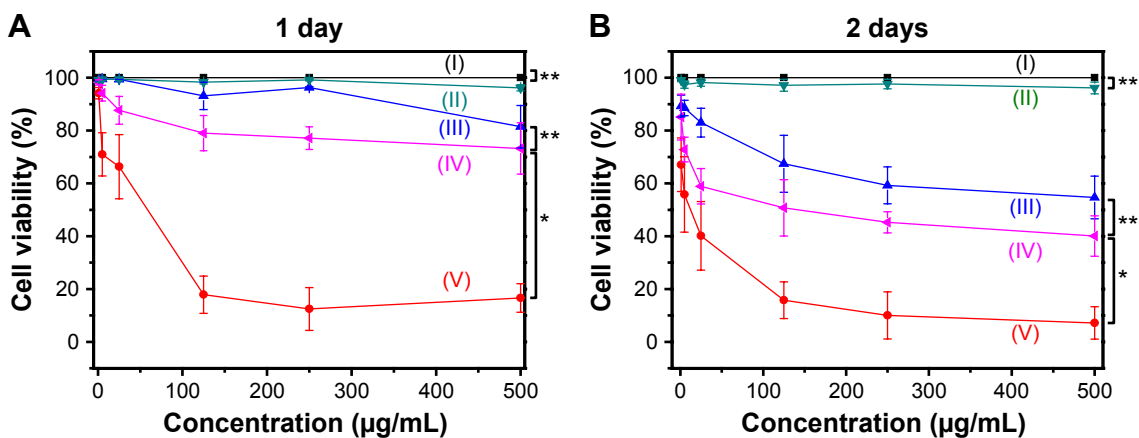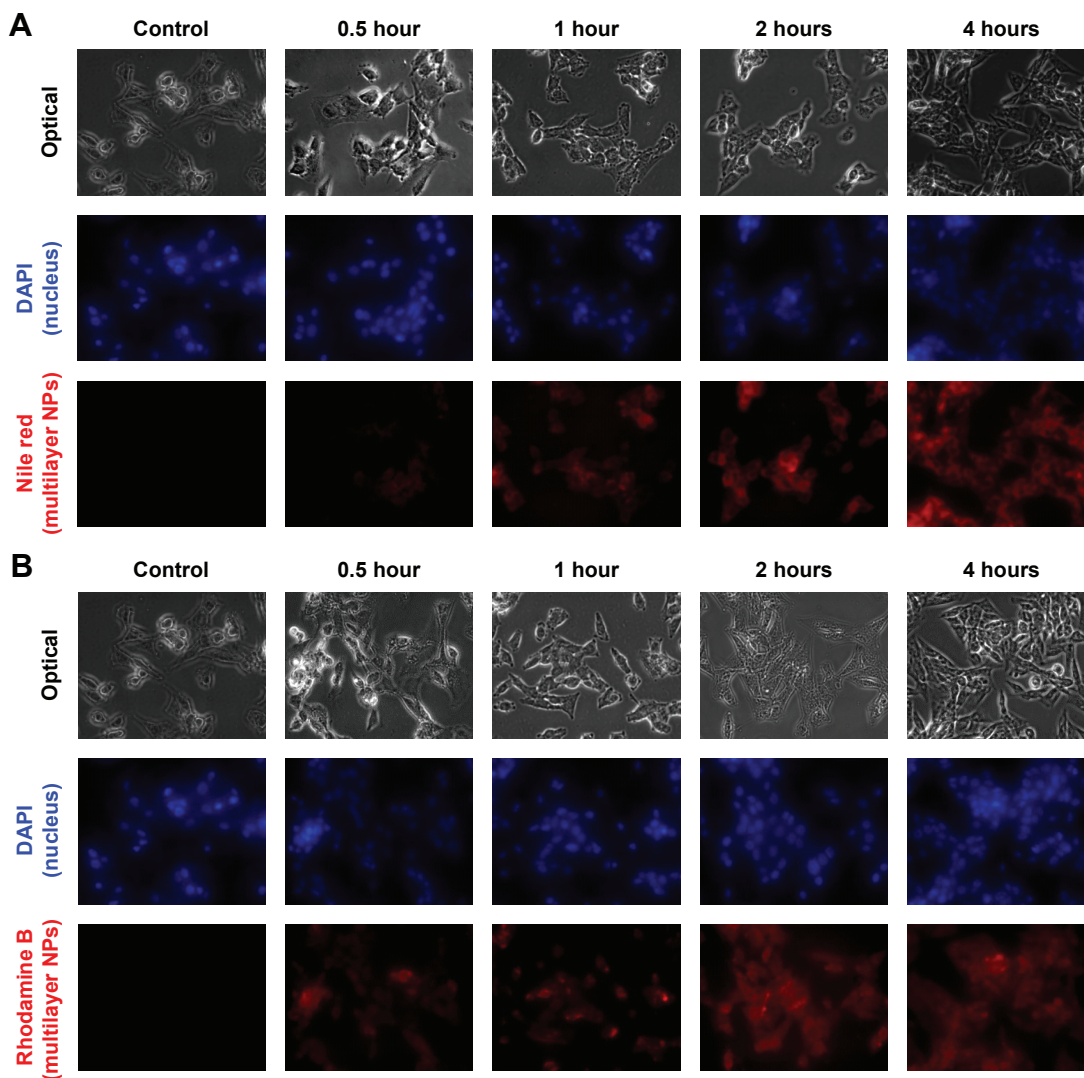**Abbreviations:** DTX, docetaxel; NPs, nanoparticles; SD, standard deviation.

Figure 6 In vitro cytotoxicity of various samples.
Notes: (**A**) Various samples, such as (I) control, (II) bare NPs, (III) the multilayer NPs, (IV) the vesicle NPs, and (V) free DTX, at 1 day and (**B**) various NPs, such as (I) control, (II) bare NPs, (III) the multilayer NPs, (IV) the vesicle NPs, and (V) free DTX, at 2 days. Data are presented as the mean ± SD (n=6). *$P>0.05$; **$P<0.05$.
Abbreviations: DTX, docetaxel; NPs, nanoparticles; SD, standard deviation.

Figure 7 Cellular uptake behavior of the multilayer NPs (magnification: ×20).
Notes: (**A**) The multilayer NPs with DTX and Nile red and (**B**) the multilayer NPs with DTX and Rhodamine B.
Abbreviations: DAPI, 4′,6-diamidino-2-phenylindole; DTX, docetaxel; NPs, nanoparticles.
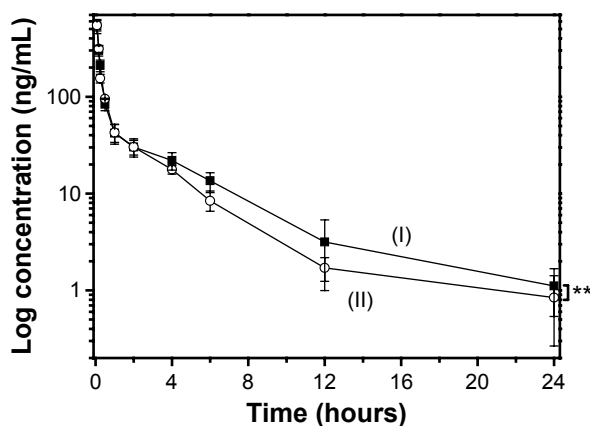
Figure 8 Mean plasma concentration–time profiles of free DTX in (I) DTX multilayer NPs and (II) Taxotere®.
Notes: Data are presented as the mean ± SD (n=5). **$P<0.05$.
Abbreviations: DTX, docetaxel; NPs, nanoparticles; SD, standard deviation.

Table 1 Pharmacokinetic parameters of the multilayer NPs

Parameters	Unit	The multilayer NPs	Free DTX
Dose	mg/kg	5 (as DTX)	5
$t_{1/2}$	h	3.9±0.5	2.5±0.4
AUC_{last}	ng·h/mL	312.6±40.9	264.3±20.3
AUC_{inf}	ng·h/mL	392.5±40.2	327.6±21.0

Notes: Data are presented as the mean ± SD (n=5). $t_{1/2}$, elimination half-life.
Abbreviations: AUC_{inf}, area under the curve from the time of zero extrapolated to infinity (predicted); AUC_{last}, area under the curve from time 0 to the last sampling time; DTX, docetaxel; NPs, nanoparticles.

circulating, and rapid cellular uptake, of the multilayer NPs in the body at a tumor site will lead to an improved therapeutic efficacy with reduced adverse side effects of DTX.

PK studies of DTX from the NPs

To support the fact that the multilayer NPs are long circulating in blood vessels, PK studies were performed (Figure 8 and Table 1). After the administration of free DTX and the multilayer NPs, $t_{1/2}$ obtained was 2.2±0.4 hours and 3.9±0.5 ng/mL, respectively. The AUC (the plasma concentration–time profile) from zero to last sampling time was 264.3±20.3 ng·h/mL and 312.6±40.9 ng·h/mL, respectively. The AUC extrapolated to infinity was 327.6±21.0 ng·h/mL and 392.5±40.2 ng·h/mL,

respectively. Based on this result, longer systemic circulation was expected with the multilayer NPs.

In vivo antitumor efficacy studies of DTX multilayer NPs in xenograft mice models

The antitumor efficacy was observed for the DTX multilayer NPs in tumor xenograft mice models (Figure 9). As controls, the mice were intravenously injected with free DTX (10 mg/kg), bare NPs, the vesicle NPs (with 10 mg/kg of DTX), or saline (200 µL). The average tumor volume was similar for all treated groups at 5 days, when the mice received the second injection. However, by 11 days, the tumor volume had increased less after treatment with DTX multilayer NPs than in mice treated with DTX in Taxotere® and the vesicle NPs, indicating that the DTX multilayer NPs were more effective in suppressing the tumor volume because of their target specificity at the tumor site. In general, NPs for high tumor target ability need a long half-life (long circulation) in blood vessels, and the hydrophilic polyethylene oxide (PEO) chain
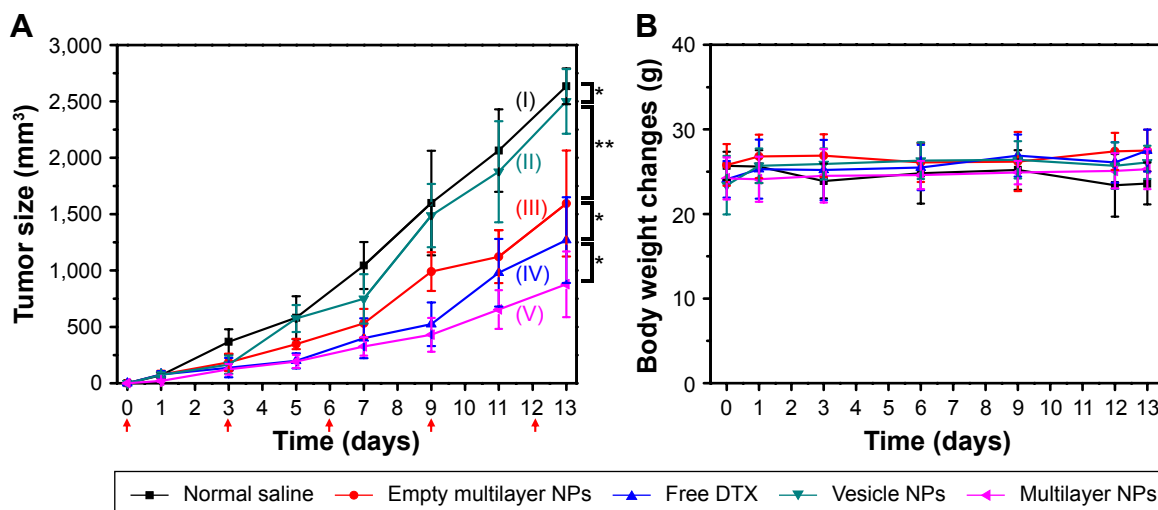

Figure 9 Therapeutic efficacy and toxicity of mice treated with various samples.
Notes: (**A**) In vivo tumor volumes after IV injection and (**B**) body weight changes. (I) Normal saline, (II) empty multilayer NPs, (III) free DTX (commercial DTX formulation [Taxotere®]), (IV) the vesicle NPs, and (V) the multilayer NPs in xenograft mice models with SCC-7 cancer cells. Red arrows indicate the injection time point. Data are presented as the mean ± SD (n=4). *$P>0.05$; **$P<0.05$.
Abbreviations: DTX, docetaxel; IV, intravenous; NPs, nanoparticles; SD, standard deviation.

in the Pluronic F-68 can enable this necessary and sufficient condition.[27–31] Also, there was no serious body weight loss in mice treated with multilayer NPs and free DTX (commercial DTX formulation [Taxotere®]) compared to that of the saline group, and the body weight of mice treated with DTX formulations gradually recovered after various treatments. Because of the presence of Pluronic F-68 on the surface of the multilayer NPs, an extended half-life of the multilayer NPs, which was also supported by PK studies, was accomplished in the systemic circulation. This led to an improved antitumor efficacy based on the enhanced permeation and retention effect.[32–34]

Conclusion

Using the vesicle fusion and the interaction between Pluronic F-68 and the lipid bilayer (the main component of vesicles), DTX Solutol nanodroplets (template NPs) were stabilized to form multilayer NPs. This led to the formation of powdery DTX formulation, which was freely dissolved in an aqueous medium. Compared with commercial DTX formulation (Taxotere®), the multilayer NPs did not contain Tween 80 (surfactant) and residual ethanol, which can cause side effects, such as leukopenia, fluid retention, nerve pain, anaphylaxis, and severe hypersensitivity. Because of the presence of Pluronic F-68 on the surface of the multilayer NPs, the extended half-life of the multilayer NPs was accomplished in the systemic circulation with an improved antitumor efficacy. Preliminary results in this study suggest that this new DTX formulation can be effectively used for cancer therapy.

Acknowledgments

Disclosure

The authors report no conflicts of interest in this work.

References

1. Liu J, Stace-Nauhton A, Jiang X, Brinker CJ. Porous nanoparticle supported lipid bilayers (protocells) as delivery vehicles. *J Am Chem Soc*. 2009;131(4):1354–1355.
2. Ramasamy T, Ruttala HB, Choi JY, et al. Engineering of a lipid-polymer nanoarchitectural platform for highly effective combination therapy of doxorubicin and irinotecan. *Chem Commun (Camb)*. 2015;51(26): 5758–5761.
3. Yuk SH, Oh KS, Koo H, Jeon K, Kim I, Kwon IC. Multi-core vesicle nanoparticles based on vesicle fusion for delivery of chemotherapic drugs. *Biomaterials*. 2011;32(31):7924–7931.
4. Lei G, MacDonald RC. Lipid bilayer vesicle fusion: intermediates captured by high-speed microfluorescence spectroscopy. *Biophys J*. 2003; 85(3):1585–1599.
5. Wang B, Zhang L, Bae SC, Granick S. Nanoparticle-induced surface reconstruction of phospholipid membranes. *Proc Natl Acad Sci U S A*. 2008;105(47):181711–181715.
6. Smith KA, Jasnow D, Balazs AC. Designing synthetic vesicles that engulf nanoscopic particles. *J Chem Phys*. 2007;127(8):84703.
7. Ramasamy T, Haidar ZS, Tran TH, et al. Layer-by-layer assembly of liposomal nanoparticles with PEGylated polyelectrolytes enhances systemic delivery of multiple anticancer drugs. *Acta Biomater*. 2014;10(12): 5116–5127.
8. Ramasamy T, Tran TH, Choi JY, et al. Layer-by-layer coated lipid-polymer hybrid nanoparticles designed for use in anticancer drug delivery. *Carbohydr Polym*. 2014;102:653–661.
9. Peyratout CS, Dähne L. Tailor-made polyelectrolyte microcapsules: from multilayers to smart containers. *Angew Chem Int Ed Engl*. 2004; 43(29):3762–3783.
10. Ochs CJ, Such GK, Yan Y, van Koeverden MP, Caruso F. Biodegradable click capsules with engineered drug-loaded multilayers. *ACS Nano*. 2010;4(3):1653–1663.
11. Sukhorukov GB, Rogach AL, Garstka M, et al. Multifunctionalized polymer microcapsules: novel tools for biological and pharmacological applications. *Small*. 2007;3(6):944–955.
12. Zhao D, Zhao X, Zu Y, et al. Preparation, characterization, and in vitro targeted delivery of folate-decorated paclitaxel-loaded bovine serum albumin nanoparticles. *Int J Nanomedicine*. 2010;5:669–677.
13. Peralta DV, He J, Wheeler DA, Zhang JZ, Tarr MA. Encapsulating gold nanomaterials into size-controlled human serum albumin nanoparticles for cancer therapy platforms. *J Microencapsul*. 2014;31(8):824–831.
14. Oh KS, Lee H, Kim JY, et al. The multilayer nanoparticles formed by layer by layer approach for cancer-targeting therapy. *J Control Release*. 2013; 165(1):9–15.
15. Alani AWG, Rao DA, Seidel R, Wang J, Jiao J, Kwon GS. The effect of novel surfactants and solutol1 HS 15 on paclitaxel aqueous solubility and permeability across a caco-2 monolayer. *J Pharm Sci*. 2010; 99(8):3473–3485.
16. Illum L, Jordan F, Lewis AL. CriticalSorb: a novel efficient nasal delivery system for human growth hormone based on solutol HS15. *J Control Release*. 2012;162(1):194–200.
17. Twelves C. Docetaxel weekly with metastatic breast cancer. *Onkologie*. 2007;30(8–9):407–408.
18. Jiang Z, Yan W, Ming J, Yu Y. Docetaxel weekly regimen in conjunction with RF hyperthermia for pretreated locally advanced non-small cell lung cancer: a preliminary study. *BMC Cancer*. 2007;7: 189–193.
19. Persohn E, Canta A, Schoepfer S, et al. Morphological and morphometric analysis of paclitaxel and docetaxel-induced peripheral neuropathy in rats. *Eur J Cancer*. 2005;41(10):1460–1466.
20. Baker J, Ajani J, Scotté F, et al. Docetaxel-related side effects and their management. *Eur J Oncol Nurs*. 2009;13(1):49–59.
21. Oh KS, Lee KE, Han SS, Cho SH, Kim D, Yuk SH. Formation of core/shell nanoparticles with a lipid core and their application as a drug delivery system. *Biomacromolecules*. 2005;6(2):1062–1067.
22. Oh KS, Han SK, Lee HS, et al. Core/shell nanoparticles with lecithin lipid cores for protein delivery. *Biomacromolecules*. 2006;7(8): 2362–2367.
23. Seo YG, Kim DW, Yeo WH, et al. Docetaxel-loaded thermosensitive and bioadhesive nanomicelles as a rectal drug delivery system for enhanced chemotherapeutic effect. *Pharm Res*. 2013;30(7): 1860–1870.
24. Gau-Racine J, Lal J, Zeghal M, Auvray L. PEO-PPO block copolymer vectors do not interact directly with DNA but with lipid membranes. *J Phys Chem B*. 2007;111(33):9900–9907.
25. Gao Y, Chen G, Weselake RJ. A rapid Nile red fluorescence-based method for triacylglycerol content in microspore-derived cell suspension cultures of *Brassica napus*. *Lipids*. 2014;49(11):1161–1188.

26. Zawad ZH. Spatial arrangement of selected fluorescence labels in lipid bilayer. *J Photochem Photobiol B*. 2013;125:26–31.

27. Oerlemans C, Bult W, Bos M, Storm G, Nijsen JF, Hennink WE. Polymeric micelles in anticancer therapy: targeting, imaging and triggered release. *Pharm Res*. 2010;27(12):2569–2589.

28. Kabanov AV, Batrakova EV, Alakhov VY. Pluronic block copolymers for overcoming drug resistance in cancer. *Adv Drug Deliv Rev*. 2002;54(5):759–779.

29. Zhang W, Shi Y, Chen Y, Hao J, Sha X, Fang X. The potential of pluronic polymeric micelles encapsulated with paclitaxel for the treatment of melanoma using subcutaneous and pulmonary metastatic mice models. *Biomaterials*. 2011;32(25):5934–5944.

30. Wang B, He X, Zhang Z, Zhao Y, Feng W. Metabolism of nanomaterials in vivo: blood circulation and organ clearance. *Acc Chem Res*. 2013;46(3):761–769.

31. Alakhova DY, Kabanov AV. Pluronics and MDR reversal: an update. *Mol Pharm*. 2014;11(8):2566–2578.

32. Matsumura Y, Maeda H. A new concept for macromolecular therapeutics in cancer chemotherapy: mechanism of tumoritropic accumulation of proteins and the antitumor agent Smancs. *Cancer Res*. 1986;46(12 pt 1):6387–6392.

33. Maeda H, Wu J, Sawa T, Matsumura Y, Hori K. Tumor vascular permeability and the EPR effect in macromolecular therapeutics: a review. *J Control Release*. 2000;65(1–2):271–284.

34. Hatakeyama H, Akita H, Harashima H. A multifunctional envelope type nano device (MEND) for gene delivery to tumours based on the EPR effect: a strategy for overcoming the PEG dilemma. *Adv Drug Deliv Rev*. 2011;63(3):152–160.